Method for Designing and Characterizing Phototherapy Shields

Tyler W. Iorizzo[1], Javed Mannan[2], and Anna N. Yaroslavsky[1*]
[1] Advanced Biophotonics Laboratory, University of Massachusetts Lowell, MA, USA
[2] University of Massachusetts Medical School, Worcester, MA, USA

*** e-mail:** anna_yaroslavsky@uml.edu

Abstract. Optimal shield properties and design are of vital importance for preventing adverse effects of light-based clinical procedures. The goal of this study was to select the most appropriate materials for a two-layer phototherapy shield. Four biocompatible fabrics, to be utilized as the layer contacting patients' skin, and two reflective materials, to be utilized as the layer facing the light source, were investigated. The optical properties of the four biocompatible fabrics and transmittance of the two reflective materials were determined in the 400–500 nm range. Absorption coefficient, scattering coefficient, and anisotropy factors of biocompatible fabrics were determined using integrating sphere spectrophotometry and an inverse Monte Carlo method. Fabric and reflective materials that exhibited highest attenuation of the blue light were selected to assemble a two-layer composite prototype. Prototypes were exposed to blue light emitted from a clinical source to ensure negligible temperature increase under clinically relevant exposure conditions. A protype blue-light phototherapy shield was made from two test materials, both of which provide sufficient light attenuation to provide patient protection. The testing method employed in this study may prove valuable for designing protective gear for a range of clinical procedures.

Keywords: phototherapy; integrating sphere spectrophotometry; phototherapy shielding.

Paper #3472 received 24 Jan 2022; revised manuscript received 09 May 2022; accepted for publication 22 Jun 2022; published online 5 Jul 2022. doi: 10.18287/JBPE22.08.030301.

1 Introduction

Side effects from various phototherapy procedures have been well documented. Blue light phototherapy for treating jaundice in neonates has been shown to cause retinal damage as well as damage to red blood cells, which may lead to bronchopulmonary dysplasia, retinopathy, and necrotizing enterocolitis [1]. Blue light phototherapy has also been associated with the formation of patent ductus arteriosus [1] and may increase the chance of melanocytic nevus development [2]. Exposure to blue light can lead to free radical generation in skin which can cause further tissue damage [3–6]. UV phototherapy for psoriasis, vitiligo, and polymorphic light eruption may lead to carcinogenesis, cataracts, lentigines, photoaging [7]. Keratitis with facial erythema has also been reported forming after UV treatments [8]. Atrophy of the superonasal iris, iris transillumination defects, pigmentation on the anterior capsule, anisocoria, and dyscoria have all been reported developing in patients receiving Intense Pulsed Light (IPL) therapy [9, 10]. Therefore, it is important to use phototherapy shields to reduce side effects from light treatments [1, 11, 12]. Shielding must protect photosensitive tissues by blocking the treatment light, while allowing the efficacious dose to be delivered over unshielded areas of the patient's body.

In this study, materials for a two-layered, blue light phototherapy shield were tested and compared. Reflective foils were considered for the top layer, facing the light source, while biocompatible fabrics were examined for the bottom layer, facing the patient.

Biocompatible fabrics were evaluated using integrating sphere spectrophotometry. Reflective materials were characterized by transmittance measurements

2 Materials and Methods

2.1 Biocompatible Fabrics

The optical properties of Spunbond Polypropylene 100 gsm, K160082 60 gsm, K170081 35 gsm, and K170087 50 gsm biocompatible fabrics (Uniquetex Engineered Nonwovens, Grover, NC, USA) were investigated using integrating sphere spectrophotometry. Seven samples were prepared for each material type. Lateral dimensions of the samples were at most 42 × 50 mm. Sample thicknesses ranged from 0.172 ± 0.004 mm to 0.306 ± 0.002 mm. Sample thickness was measured using a digital micrometer (293–340 Digital Micrometer, Mitutoyo, Japan).

2.2 Reflective Foils

Reflective foils DM146 and DE 050 (Dunmore, Bristol, PA, USA) were compared using transmittance spectrophotometry. Seven samples with lateral dimensions 45 × 12 mm were prepared for each foil. Average thicknesses of DM146 and DE 050 samples were 0.021 ± 0.001 mm and 0.082 ± 0.001 mm, respectively. Thicknesses were measured using a micrometer (293–340 Digital Micrometer, Mitutoyo, Japan).

2.3 Integrating Sphere Spectrophotometry

A single integrating sphere system that was used to measure the total transmittance, diffuse transmittance, and diffuse reflectance of the biocompatible fabrics in the spectral range of 400–500 nm is shown in Fig. 1. Samples were placed at the entrance and exit ports of the integrating sphere (4P-GPS-033-SL, Labsphere, North Sutton, NH, USA) for transmittance and reflectance measurements, respectively. Light from a halogen lamp (HL-2000, 360–2000 nm, Ocean Optics, Dunedin, FL, USA) was focused onto the samples. The focal spot had a diameter of 3 mm. Sample and exit ports of the integrating sphere had a diameter of 14 mm and 25.4 mm, respectively. Transmittance through air, and reflectance from Spectralon (> 99% reflectance) were used as a reference. The exit port of the integrating sphere was opened during diffuse transmittance measurements to allow collimated light to escape. Collimated transmittance was calculated by subtracting diffuse transmittance from total transmittance at each wavelength investigated. An HR2000 spectrometer (Ocean Optics, Dunedin, FL, USA) was coupled to the auxiliary port of the integrating sphere via an optical fiber (P600-2-SR, Ocean Optics, Dunedin, FL, USA) to measure the spectral response in the 400–500 nm range.

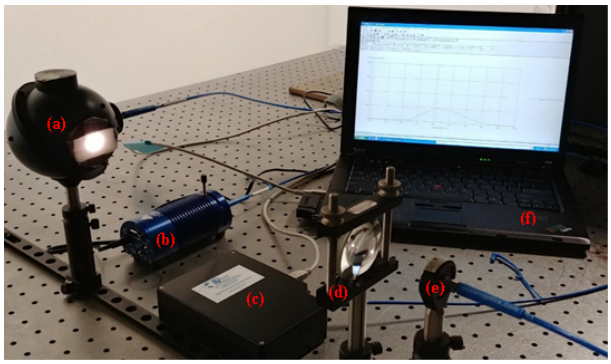

Fig. 1 Integrating sphere set-up. Halogen lamp light (b) was coupled into an optical fiber (e) and focused onto the sample by a lens (d). Light transmitted and reflected from the sample was collected by the integrating sphere (a) and detected by a grating spectrometer (c). Data acquisition was controlled by external PC (f).

2.4 Inverse Monte Carlo Technique

Absorption coefficients, scattering coefficients, and anisotropy factors of the biocompatible fabric materials were calculated from measured quantities under an assumption of Henyey-Greenstein scattering phase function [13] using an inverse hybrid Monte Carlo algorithm [14]. This method employed a forward Monte Carlo technique that accounted for the exact geometrical and optical properties of the integrating sphere walls and light losses at the edges of the samples. The forward Monte Carlo method was integrated into a Quasi-Newton inverse algorithm [15], optimized to reduce the number of forward Monte Carlo calls.

2.5 Transmittance Measurements

Transmittance through reflective materials in the spectral range of 400–500 nm was measured using a spectrophotometer (Lambda 1050, PerkinElmer Inc., Waltham, MA, USA). The spectrophotometer slit width was set to 5 nm, and the wavelength step size was set to 2 nm. The illumination beam had a diameter of 4.5 mm. Transmittance through air was used as a reference. Transmittance of each reflective sample were measured twice, then averaged.

2.6 Temperature Monitoring

After determining the optical properties and selecting appropriate biocompatible and reflective materials, a two-layer shield prototype was assembled. The temperature of the composite shield exposed to 450–470 nm light was monitored over a 48-hour time interval. The experimental arrangement used for monitoring the temperature of the shield is shown in Fig. 2. A Natus neoBLUE mini LED phototherapy lamp (Natus Medical Incorporated, San Carlos, CA, USA) was used as a light source. Shield samples were suspended above the optical table to provide thermal isolation. The lamp was placed 30.5 cm above the samples. At this height, samples were exposed to a peak central intensity of 30 $\mu W/cm^2/nm$. A

temperature sensor was attached to the biocompatible surface of the composite shield, where the shield would be in contact with patient skin. The sensor was connected to an external temperature monitor (CT16A2080-948, Minco, Minneapolis, MN, USA). The geometry and duration of temperature monitoring experiments were exactly as those during the clinical phototherapy procedure.

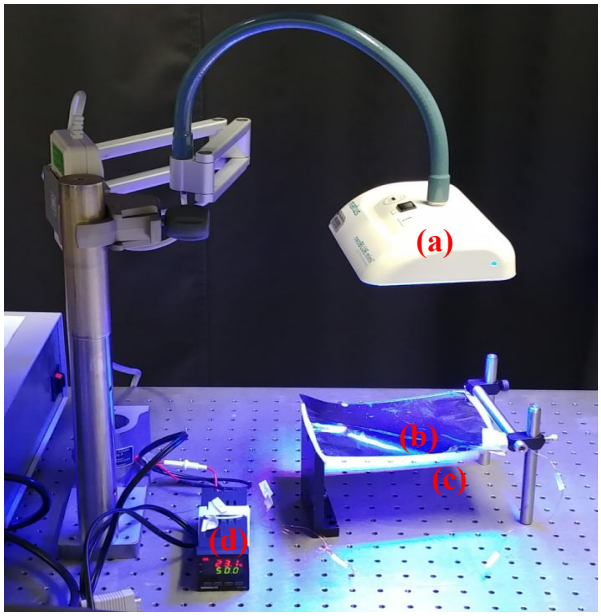

Fig. 2 Experimental setup used for shield material temperature monitoring. Light from the phototherapy lamp (a) was incident onto the shield material (b). A temperature sensor (c) underneath the sample allowed the temperature monitor (d) to measure the temperature of the sample.

3 Results

3.1 Optical Properties of Biocompatible Fabric Materials

Absorption coefficients, scattering coefficients, and anisotropy factors of biocompatible fabric materials, determined in the spectral range of 400–500 nm, are shown in Fig. 3. Absorption coefficients are presented in Fig. 3(a). Absorption of Spunbond Polypropylene 100 gsm, K170081 35 gsm, and K170087 50 gsm monotonously increase with increasing wavelength. The absorption spectrum of K160082 60 gsm decreases with increasing wavelength between 400–420 nm, then increases with wavelength in the 420–500 nm range. K160082 60 gsm exhibited the greatest absorption out of all biocompatible fabrics investigated, ranging between 0.4 and 0.1 mm^{-1} over the entire spectral range. The absorption of all other fabrics was less than 0.09 mm^{-1}.

Scattering coefficients are shown in Fig. 3(b). Scattering of all fabrics decreased with increasing wavelength. K160082 60 gsm has the greatest scattering over the entire spectral region, with coefficients greater than 7.3 mm^{-1}. All other fabrics have scattering less than 4.6 mm^{-1}.

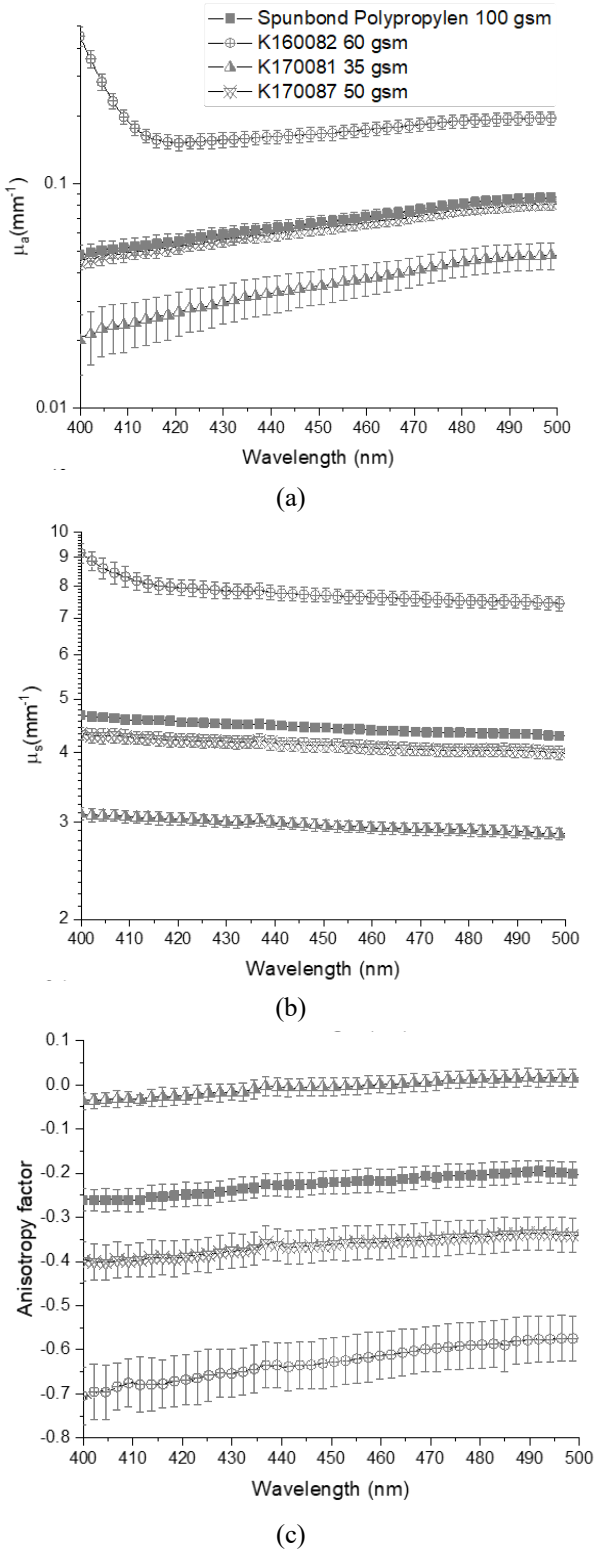

Fig. 3 Absorption coefficients (a), scattering coefficients (b), and anisotropy factors (c) of biocompatible fabric materials between 400–500 nm. Squares – Spunbond Polypropylene 100 gsm. Circles with a Cross – K160082 60 gsm. Half-filled Upright Triangle – K170081 35 gsm. Upside-down Triangle with an X – K170087 50 gsm. Bars – standard deviations.

Anisotropy of Spunbond Polypropylene 100 gsm, K160082 60 gsm, and K170087 50 gsm are negative over the entire spectral range, whereas K170081 35 gsm has positive values between 458-500 nm. K160082 60 gsm has the greatest negative anisotropy factors ranging between –0.7 and –0.65 over the investigated spectral region.

Of the four biocompatible fabrics investigated, K160082 60 gsm has the greatest absorption and scattering in the 400–500 nm spectral range. The results show that scattering is the dominant attenuation process. Calculated absorption coefficients are an order of magnitude lower than the scattering coefficients. Due to the low absorption, a low temperature increase in the fabric during treatment can be expected. Moreover, K160082 60 gsm has the largest negative anisotropy factors out of the four fabrics tested. Thus, light has the highest probability of exhibiting backscattering when incident on K160082 60 gsm. Due to predominant backscattering properties of the K160082 60 gsm, more light will propagate towards the light source as compared to towards the patient. These results indicate that out of the four biocompatible fabrics tested, K160082 60 gsm is the most appropriate material for the bottom layer of the blue light phototherapy shield.

3.2 Transmittance Measurements of Reflective Materials

Transmittance of the two reflective materials were below 0.1% over the entire 400–500 nm range. Average transmittance measurements ranged between 0.039–0.071%, and 0.024–0.045% for Dm146 and DE 050, respectively. Lower transmittance points to higher attenuation of 400–500 nm light by DE 050 as compared to Dm146. Therefore, DE 050 was selected for the top layer of the blue light phototherapy shield.

3.3 Temperature Monitoring of Selected Shielding Materials

Based on the results of the optical experiments, composite shields were prepared with DE 050 as the top layer facing the light and K160082 60 gsm as the bottom layer facing patient's skin. Recorded shield temperatures ranged between 16.3 °C and 23.3 °C when exposed to blue treatment light. Temperatures of the shields followed the same temperature trends as room temperature. Thus, the phototherapy lamp did not have a significant effect on the shield temperature.

4 Discussion

Many studies have been made to characterize and compare shielding materials. The most common approach is to measure optical transmission of the shields in the spectral range of interest. Chin et al. [16] had investigated the transmission of 250–800 nm light through 12 potential eye shields using a spectrophotometer system. Robinson et al. [17] measured the transmission of 300–750 nm light through three eye shield materials while placed in phototherapy units, to account for reflection from the therapy unit walls. Otman et al. [18] determined the UV transmission of commercial sunglasses and contact lenses that were allowed to be worn by patients during treatments using a spectrophotometry system. Abdulla et al. [19] measured UV transmission through potential shielding materials for genital protection from UVA, broad band UVB, and narrow band UVB illumination. In this paper we explored a more general approach that can be utilized not only for testing and comparing prospective shields, but also to inform their selection, optimization, and design. Since attenuation of light is governed by the optical properties of the medium, we started with determining the absorption coefficients, scattering coefficients, and anisotropy factors of the materials from diffuse reflectance and transmittance measurements using integrating sphere spectrophotometry [20–23] and inverse Monte Carlo technique. This approach enables comparison of the shield attenuation properties irrespectively of the material thickness and allows for its optimization without exhaustive repetitive transmission measurements.

Each layer of the designed shield provides sufficient protection from therapeutic blue light. While the reflective top layer exhibits low transmittance in this spectral range, it may increase in temperature when illuminated and may have sharp edges which may injure the patient. The biocompatible fabric bottom layer protects the patient from any harm caused by the foil and allows the shield to conform to the patient's body to provide a secure fit. Total attenuation per mm thickness of the fabric can be found from the characterized optical properties. Fabric thickness can then be optimized to provide adequate protection from the treatment light in case the top layer fails. The top layer of this shield will reflect treatment light away from the patient, which may be harmful for other individuals in the treatment room [3–6]. Reflection can be reduced by adding another fabric layer on top of the reflective material, thus resulting in a three-layered shield.

5 Conclusion

Selecting shielding materials based on its optical and thermal properties enables straightforward optimization of shield design and ensures proper patient protection during phototherapy. While this study focused on shielding for blue light phototherapy, this method for characterizing shield materials can be utilized for any desired wavelength range and phototherapy procedure.

Disclosures

The authors have stated explicitly that there are no conflicts of interest in connection with this article.

Acknowledgments

We would like to thank Cheryl Gomes from the Fabric Discovery Center at the University of Massachusetts

Lowell for providing the test materials for this study and Androniki Mitrou from the Advanced Biophotonics Laboratory for assistance with temperature measurements. Funding provided by the Office of Technology Commercialization is greatly appreciated.

References

1. L. A. Stokowski, "Fundamentals of Phototherapy for Neonatal Jaundice," Advances in Neonatal Care 11(5S), S10–S21 (2013).
2. Z. Csoma, E. Tóth-Molnár, K. Balogh, H. Polyánka, H. Orvos, H. Ócsai, L. Kemény, M. Széll, and J. Oláh, "Neonatal Blue Light Phototehrapy and Melanocytic Nevi: A Twin Study," Pediatrics 128(4), e856–e864 (2011).
3. B. F. Godley, F. Shamsi, F.-Q. Liang, S. G. Jarrett, S. Davies, and M. Boulton, "Blue Light Induces Mitochondrial DNA Damage and Free Radical Production in Epithelial Cells," Journal of Biological Chemistry 280(22), 21061–21066 (2005).
4. S. Vandersee, M. Beyer, J. Lademann, and M. E. Darvin, "Blue-Violet Light Irradiation Dose Dependently Decreases Carotenoids in Human Skin, Which Indicates the Generation of Free Radicals," Oxidative Medicine and Cellular Longevity 2015, 579675 (2015).
5. Y. Nakashima, S. Ohta, and A. M.Wolf, "Blue light-induced oxidative stress in live skin," Free Radical Biology and Medicine 108, 300–310 (2017).
6. J. G. Coats, B. Maktabi, M. S. Abou-Dahech, and G. Baki, "Blue Light Protection, Part 1 – Effects of blue light on the skin," Journal of Cosmetic Dermatology 20(3), 714–717 (2021).
7. S. A. Holme, A. V. Anstey, "Phototherapy and PUVA photochemotherapy in children," Photodermatology Photoimmunology and Photomedicine 20(2), 69–75 (2004).
8. P. Komericki, P. Fellner, Y. El-Shabrawi, and N. Ardjomand, "Keratopathy after ultraviolet B phototherapy," Wiener Klinische Wochenschrift 117(7–8), 300–302 (2005).
9. G. Javey, S. G. Schwartz, and T. A. Albini, "Ocular Complication of Intense Pulsed Light Therapy: Iris Photoablation," Dermatologic Surgery 36(9), 1446–1468 (2010).
10. M. Crabb, W. O. Chan, D. Taranath, and S. C. Huilgol, "Intense pulsed light therapy (IPL) induced iritis following treatment for a medial canthal capillary malformation," Australasian Journal of Dermatology 55(4), 289–291 (2014).
11. W. Rosenfield, S. Sadhev, V. Brunot, R. Jhaveri, I. Zabaleta, and H. E. Evans, "Phototherapy Effect on the Incidence of Patent Ductus Arteriosus in Premature Infants: Prevention With Chest Shielding," Pediatrics 78(1), 10–14 (1986).
12. H. S. Kim, E.-K. Kim, H.-E. Lee, Y.-K. Lee, C.-H. Park, K.-R. Park, J.-D. Park, B.-I. Kim, W.-H. Kim, J.-H. Choi, Y.-S. Yun, C.-K. Yun, and J.-M. Lee, "Influence of Phototherapy on Incidence of Patent Ductus Arteriosus in Very Low Birth Weight Infants," Journal of the Korean Pediatric Society 40(10), 1410–1418 (1997).
13. L. G. Henyey, J. L. Greenstein, "Diffuse radiation in the Galaxy," Astrophysical Journal 93, 70–83 (1941).
14. I. V. Yaroslavsky, A. N. Yaroslavsky, T. Goldbach, and H.-J. Schwarzmaier, "Inverse hybrid technique for determining the optical properties of turbid media from integrating-sphere measurements," Applied Optics 35(34), 6797–6809 (1996).
15. J. E. Dennis, R. B. Schnabel, Numerical Methods for Unconstrained Optimization and Nonlinear Equations, Prentice-Hall, Upper Saddle River (1983).
16. K. C. Chin, M. J. Moseley, and S. C. Bayliss, "Light transmission of phototherapy eyeshields," Archives of Disease in Childhood 62, 970–971 (1987).
17. J. Robinson, M. J. Moseley, A. R. Fielder, and S. C. Bayliss, "Light transmission measurements and phototherapy eyepatches," Archives of Disease in Childhood 66, 59–61 (1991).
18. S. G. H. Otman, L. D. El-Dars, C. Edwards, E. Ansari, D. Taylor, B. Gambles, I. Chalmers, and A. V. Anstey, "Eye protection for ultraviolet B phototherapy and psoralen ultraviolet A patients," Photodermatology Photoimmunology and Photomedicine 26(3), 143–150 (2010).
19. F. R. Abdulla, C. Breneman, B. Adams, and D. Breneman, "Standards for genital protection in phototherapy units," Journal of the American Academy of Dermatology 62(2), 223–226 (2010).
20. S. L. Jacques, M. O. Gaeeni, "Thermically induced changes in optical properties of heart," Images of the Twenty-First Century. Proceedings of the Annual International Engineering in Medicine and Biology Society 4, 1199–1200 (1989).
21. A. N. Yaroslavsky, P. C. Schulze, I. V. Yaroslavsky, R. Schober, F. Ulrich, and H.-J. Schwarzmaier, "Optical properties of selected native and coagulated human brain tissues in vitro in the visible and near infrared spectral range," Physics in Medicine & Biology 47(12), 2059–2073 (2002).
22. A. N. Bashkatov, E. A. Genina, V. I. Kochubey, and V. V. Tuchin, "Optical properties of human skin, subcutaneous and mucous tissues in the wavelength range from 400 to 2000 nm," Journal of Physics D: Applied Physics 38, 2543 (2005).
23. E. Salomatina, B. Jiang, J. Novak, and A. N. Yaroslavsky, "Optical properties of normal and cancerous human skin in the visible and near-infrared spectral range," Journal of Biomedical Optics 11(6), 064026 (2006).